Transitional behavior in hydrodynamically coupled oscillators

S. Box and L. Debono
H.H. Wills Physics Laboratory, University of Bristol, Tyndall Avenue, Bristol, BS8 1TL, U.K.

D. B. Phillips
Department of Physics and Astronomy, University of Glasgow, Glasgow G12 8QQ, Scotland, U.K.

S. H. Simpson*
ASCR, Institute of Scientific Instruments, Kràlovopolskà 147, 612 64 Brno, Czech Republic
(Received 5 November 2014; revised manuscript received 27 January 2015; published 17 February 2015)

In this article we consider the complete set of synchronized and phase-locked states available to pairs of hydrodynamically coupled colloidal rotors, consisting of spherical beads driven about circular paths in the same, and in opposing senses. Oscillators such as these have previously been used as coarse grained, minimal models of beating cilia. Two mechanisms are known to be important in establishing synchrony. The first involves perturbation of the driving force, and the second involves deformation of the rotor trajectory. We demonstrate that these mechanisms are of similar strength, in the regime of interest, and interact to determine observed behavior. Combining analysis and simulation with experiments performed using holographic optical tweezers, we show how varying the amplitude of the driving force perturbation leads to a transition from synchronized to phase-locked states. Analogies with biological systems are discussed, as are implications for the design of biomimetic devices.

DOI: 10.1103/PhysRevE.91.022916 PACS number(s): 05.45.Xt, 05.40.Jc, 83.10.Mj, 37.10.Vz

I. INTRODUCTION

Synchronization is ubiquitous in driven assemblies of weakly coupled oscillators, with sufficiently similar natural frequencies [1,2]. It apparently transcends length scales and physical context, arising in the rotational dynamics of magnetic stars [3] as well as in the flight paths of subatomic particles, in the Large Hadron Collider [4], and as an emergent, sociological effect observable in traffic flow [5] or financial trading [6]. In microbiology synchronization is of fundamental importance. Beating cilia generate relative fluid flow that can be used either for propulsion [7], in the case of swimming algae and other microorganisms, or for fluid transport in mammalian digestive or respiratory tracts [8]. Biological function is often accompanied by synchronization, which appears to arise spontaneously, and may be associated with increased efficiency [9–11]. While synchronization is known to depend on weak coupling, the details of the relevant interactions and underlying mechanisms are subject to ongoing inquiry, especially in biological systems. Fields of cilia exhibit metachronal coordination in which adjacent cilia beat with a constant phase lag [12,13], while the flagella of the alga Chlamydamonous admit several distinct states of synchronization [14–16]. In the former case, the coordinating interaction is thought to be hydrodynamic [17,18]; in the latter, mechanical [19,20], involving rotation of the swimmer body [19], although this does not fully describe the occurrence of the discrete modes, or switching between them.

In this article, attention is restricted to the phenomena that may be produced by hydrodynamic interactions alone. We consider the complete set of steady-state modes available to pairs of coupled colloidal rotors, circulating in the same, and in opposing senses. As described at greater length below, each of these arrangements is shown to sustain two distinct modes, in which the rotors reach a stable steady state. These we refer to, generically, as modes, states, or equilibria (applying the last term in the dynamical, not thermodynamical sense; these systems are obviously not at thermodynamic equilibrium). Each equilibrium is characterized by a particular relationship between the rotor phases. For example, we say that a pair of rotors, circulating in the same sense, with zero phase difference, are synchronized and refer to other phase differences as phase locked.

Hydrodynamic synchronization requires the breaking of time-reversal symmetry [21–23]. As has recently been shown, this can result from fluid compressibility [23]. As noted by the authors, the resulting effects are marginal for the regime in which flagellae and cilia operate. Here, the dominant mechanisms are thought to rely on the incorporation of additional degrees of freedom. Accordingly, two purely hydrodynamic synchronization mechanisms, effective for incompressible fluids at low Reynolds number, have been described previously. They rely, respectively, on elastic deformation of the rotor trajectories and driving force modulation [24–26]. Employing a combination of analysis, simulation, and experiments, using holographic optical tweezers (HOT), we show these processes acting either competitively or cooperatively to determine the observed behavior. In particular, a transition between synchronized and phase-locked states is induced by varying the strength of the force modulation.

Our principle aim is to understand the transition between synchronization and phase locking in this class of hydrodynamically coupled oscillator. However, analogies to real, biological systems are evident, suggesting that even when correlations in the motion are not principally determined by hydrodynamics, they may act in cooperation with it. For instance, the equilibrium states of our counter-rotating rotors

*simpson@isibrno.cz

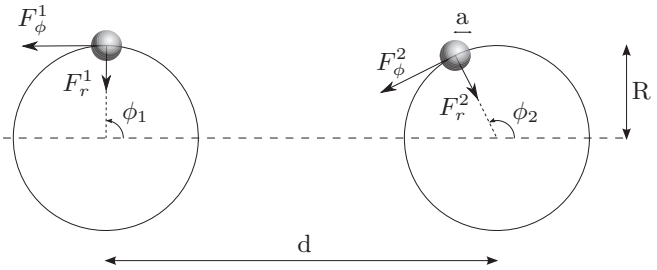

FIG. 1. Schematic showing the geometric arrangement and parameters defining the system of colloidal rotors.

are seen to be reminiscent of the swimming strokes of the alga Chlamydamonus. In addition, our comments on the efficiency of the various states, and on methods to strengthen and reinforce synchronization, may have implications for the design and control of artificial microfluidic elements.

II. MODEL SYSTEM

We consider a pair of colloidal oscillators each represented by a single spherical bead, driven by a tangential force, about a circular trajectory to which it is harmonically bound (see Fig. 1). Similarly reduced models have been employed, both theoretically [9,11,24,25,27,28] and experimentally [21,26], to investigate hydrodynamic synchronization of beating cilia. The apparently crude approximation of complex elements, such as cilia, by colloidal beads is partially justified by the near equivalence of the flow fields generated by real and model systems [29,30]. Regardless of the fidelity with which the biological systems are represented, this coarse-grained analog serves as an archetypal model of hydrodynamic synchronization that is of basic interest as well as being of relevance to the design of future biomimetic, microfluidic devices, such as the magnetic cilia studied by Shields *et al.* [31].

The model [Fig. (1)] is parametrized by a radial stiffness, k_r, binding the bead, of radius a, to a circular path of radius R_0. The bead is driven by a weakly phase-dependent tangential force, $F_\phi^i(\phi)$ (where $i = 1,2$ labels the rotor). The separation between the centers of rotation is d.

Previous work has concentrated on rotors circulating in the same sense $[F_\phi^1(\phi) = F_\phi^2(\phi)]$, and has revealed two distinct mechanisms leading to synchronization.

First, when the tangential force is constant, and independent of phase, the finite value of the radial stiffness, k_r, allows elastic distortions of the bead trajectories, which can result in synchronization. Since the tangential force depends only on the angular coordinate, ϕ, reducing the radius of the path increases the angular velocity. In this way, phase differences arising between the beads are reduced as the leading bead is pushed outwards and the trailing bead pulled inwards, until synchrony is restored. This effect appears always to induce synchronization, as opposed to phase locking.

Second, a weak phase dependence to the tangential force can also, through subtler considerations [25], lead to synchronization. Qualitatively, a small phase difference between a pair of beads will be reduced in regions of the cycle in which the force is decreasing with phase (since the trailing bead feels a greater force than the leading one), and grow in regions where the force increases with phase. Hydrodynamic interactions can modify the rate of progress of the bead about its path, resulting in systematic reductions of phase differences over a complete cycle and leading, once more, to synchrony. It has previously been suggested that this mechanism is of longer range than the one based on finite k_r and dominates in the far field [25].

In this work, we consider pairs of colloidal rotors of this type driven by tangential forces of the general form given in Eq. (1):

$$F_\phi^i(\phi) = F_0^i[1 - A^i \sin(2\phi)], \tag{1}$$

where $i = 1,2$ labels the rotor. Restriction of the phase dependence of the force to the second harmonic implies no particular loss of generality since the first harmonic is ineffective to first order, and the influence of higher-order terms becomes progressively weaker [26]. We further consider pairs of oscillators of even parity $[F_\phi^1(\phi) = F_\phi^2(\phi)$, i.e., $F_0^1 = F_0^2$, $A^1 = A^2]$, in which rotors circulate in the same sense, as well as odd parity $[F_\phi^1(\phi) = -F_\phi^2(\pi - \phi)$, i.e., $F_0^1 = -F_0^2$, $A^1 = -A^2]$, in which rotors circulate in opposing senses. In each case, we examine the effect of varying the amplitude of the perturbation, A^i, between negative and positive values.

In the following sections, this system is analyzed algebraically, numerically, and experimentally, using holographically controlled optical traps to apply appropriate forces to pairs of polystyrene beads. The complete set of steady-state modes available to this system are presented, and the mechanisms underlying their stability are elucidated.

III. THEORETICAL

In the low Reynolds number limit, the equation of motion for two externally driven spherical particles is

$$\mathbf{F}_i = \sum_j \mathbf{H}_{ij}^{-1}\dot{\mathbf{r}}_j + \mathbf{f}_i(t), \tag{2}$$

where $i = 1,2$ is the bead index, $\mathbf{F}_i$ is the external driving force on rotor i, and $\dot{\mathbf{r}}_i$ is its velocity. $\mathbf{H}$ is the mobility matrix given here by the Oseen tensor [32]. $\mathbf{f}_i$ is the stochastic Langevin force, uncorrelated, with zero mean, $\langle \mathbf{f}_i \rangle = 0$, and covariance, $\langle \mathbf{f}_i(t) \otimes \mathbf{f}_i(t') \rangle = 2k_B T \mathbf{H}_{ij}^{-1} \delta(t - t')$. We assume small, distant rotors ($a \ll d$, $R \ll d$), moving in one another's hydrodynamic far-field; in subsequent equations, terms beyond $\mathcal{O}(\frac{a}{d})$ and $\mathcal{O}(\frac{R}{d})$ are discarded. Neglecting thermal fluctuations, and following the procedure described in detail in Ref. [26] (see Sec. 2, Supplemental Material), evolution of the radial coordinate of each bead can be assumed instantaneous on the time scale of the phase evolution, thereby decoupling angular and radial components. Equations of motion for the phases of the rotors result:

$$\dot{\phi}_i = \frac{F_\phi^i(\phi_i)}{\gamma R_0} + \frac{3a}{8\gamma R_0 d}\Bigg\{ F_\phi^j(\phi_j)[3\cos(\phi_i - \phi_j) - \cos(\phi_i + \phi_j)] - \frac{F_\phi^i(\phi_i) F_\phi^j(\phi_j)}{R_0 k_r}[3\sin(\phi_i - \phi_j) - \sin(\phi_i + \phi_j)]\Bigg\}, \tag{3}$$

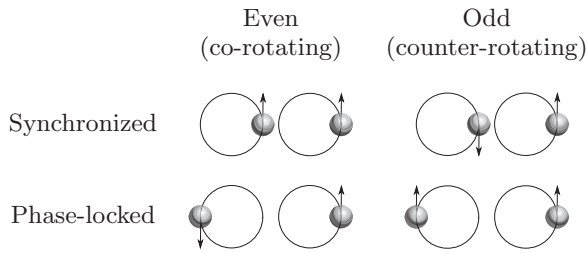

FIG. 2. Schematic indicating the motion of the beads in the synchronized and phase-locked states of pairs of rotors of even (corotating) and odd (counter-rotating) parity.

for $i = 1,2$, and $\dot{\phi}$ is the time derivative of the phase. $\gamma = 6\pi\mu a$ is the Stokes drag on an isolated sphere. In order to identify equilibria and assess their stability, we next consider the evolution of small disturbances. The deviation in the relative phase of the rotors, with respect to a particular equilibrium, is given by Eq. (4):

$$\delta^{E/O} = (\phi_1 \mp \phi_2) - \delta_0^{E/O}. \tag{4}$$

Here, the superscript E refers to even, or same sense rotation, for which the phase difference is taken, and O is odd, or opposing sense rotation, which makes use of the phase sum. $\delta_0^{E/O}$ is an equilibrium state, $\delta_0^{E/O} = (\phi_1 \mp \phi_2)_{\text{eqm}}$. Equation (3) can be used to evaluate the time rate of change of a disturbance, $\dot{\delta}^{E/O}$, for small $\delta^{E/O}$. The condition that a particular pair of phases, $\delta_0^{E/O}$, correspond to an equilibrium, is simply that $\dot{\delta}^{E/O} \propto \delta^{E/O}$, so that $\delta^{E/O}(t) = 0$ is a solution. Precisely four equilibrium states emerge; see Fig. 2.

The first two we refer to as synchronized, as indicated by the subscript S. In this case the sum, or difference, of the rotor phases is zero, $\delta_0^{E/O} = 0$, depending on the parity of the rotors. The second two are referred to as phase-locked, or antisynchronized, the phases being related by $\delta_0^{E/O} = \pi$ (where the subscript P refers to the phase locked state).

A strong condition for the stability of a particular state is simply that the time rate of change of a small disturbance be of opposite sign to the disturbance itself, i.e., that $\dot{\delta}/\delta < 0$, for all phase angles, ϕ. Applying Eq. (3) to each equilibrium state, and assuming $\delta^{E/O} \ll 1$, gives

$$\frac{\dot{\delta}^E_{S/P}}{\delta^E_{S/P}} \approx -\frac{2F_0^1 A^1 \cos(2\phi)}{\gamma R_0} \mp \frac{3a}{4d}\left\{\frac{3\left(F_0^1\right)^2[1 - A^1\sin(2\phi)]^2}{4R_0^2\gamma k_r} - \frac{F_0^1 A^1\cos(2\phi)}{\gamma R_0}[3 - \cos(2\phi)]\right\}, \tag{5a}$$

$$\frac{\dot{\delta}^O_{S/P}}{\delta^O_{S/P}} \approx -\frac{2F_0^1 A^1 \cos(2\phi)}{\gamma R_0} \mp \frac{3a}{4d}\left\{\frac{\left(F_0^1\right)^2[1 - A^1\sin(2\phi)]^2}{R_0^2\gamma k_r} + \frac{F_0^1 A^1\cos(2\phi)}{\gamma R_0}[3\cos(2\phi) - 1]\right\}. \tag{5b}$$

Here, ϕ, is the phase of the unperturbed system, e.g., for the synchronized state of even parity rotors, $\delta_S^E = \phi_1 - \phi_2$, and we have used $\phi_1 = \delta_S^E + \phi$, $\phi_2 = \phi$.

These equations are revealing, although the appearance of the first terms [the zeroth-order terms in (a/d)] on the right-hand sides of Eqs. (5a) and (5b) is, perhaps, misleading. These terms occur for rotors even in the absence of hydrodynamic interaction and arise solely by virtue of the force modulation. When the force is decreasing with phase [$\cos(2\phi) < 0$], trailing beads experience higher tangential forces than leading ones, thereby closing the gap. Conversely, when it is increasing, the opposite occurs. For this term to contribute to stability, its time average over a complete cycle would need to be negative, which is possible if circulation is slower in some parts of the cycle than in others. However, since the angular average is zero, the effect, if it exists, is likely to be minimal.

Next, the first-order terms in (a/d) contain two contributions. The first is of the same sign for all phase angles, ϕ. It continues to act when the tangential force is constant ($A^1 = 0$) and vanishes when the radial stiffness is infinite. It can therefore be identified with elastic trajectory deformation (finite k_r), although its strength is modified for phase-dependent force ($A^1 \neq 0$). It always promotes the stability of synchronized states and degrades the stability of phase locking. The second contribution to the first-order term is effective only when the force varies with phase but appears even for rigidly tethered rotors ($k_r = \infty$). Unlike the first contribution, the sign of the second varies with phase. This time its angular average does not vanish, so that it may be expected to influence synchronization. In all cases, positive values of A^1 promote synchronization.

Evidently, the only states that are potentially stable under the strong condition that $\dot{\delta}^{E/O}/\delta^{E/O} < 0 \forall \phi$, are the synchronized states, since they are stabilized by the first components of the first-order terms in Eq. (5) and these are of the same sign for all values of ϕ. However, other states may be stable in a weaker sense; for example, the requirement that disturbances [Eq. (4)] be reduced over a complete cycle. This looser condition allows $\dot{\delta}^{E/O}/\delta^{E/O}$ to vary in sign over a cycle, providing that negative contributions outweigh positive. Synchronized states, for which the two first-order terms are comparable, due to particular values of stiffness, k_r, or force amplitude, A^1, may only be stable under the weak condition. Crucially, it is the only sense in which the phase-locked states, identified above, can be stable.

Defining the *synchronization strength* as the cycle averaged growth of a disturbance from equilibrium results in the less exacting stability condition

$$\Gamma^{E/O}_{S/P} = \int_0^{2\pi} \frac{\dot{\delta}^{E/O}_{S/P}}{\delta^{E/O}_{S/P}\dot{\phi}} d\phi < 0, \tag{6}$$

where $\Gamma^{E/O}_{S/P}$ is the synchronization strength of the indicated mode and is negative for stable states; i.e., stability requires that the growth of the cycle averaged phase difference is decreasing. Using Eq. (5) and, following Ref. [26], taking $\delta^{E/O}_{S/P} = 0$ in Eq. (3) to get appropriate expressions for $\dot{\phi}$ for each equilibrium state gives

$$\Gamma^E_{S/P} = \mp\frac{3\pi a}{2d}\left\{\frac{3F_0^1}{R_0 k_r} + \frac{2}{A^1}[1 - \sqrt{1 - (A^1)^2}]\right\} \tag{7a}$$

$$\Gamma^O_{S/P} = \mp\frac{3\pi a}{2d}\left\{\frac{F_0^1}{R_0 k_r} + \frac{6}{A^1}[1 - \sqrt{1 - (A^1)^2}]\right\}. \tag{7b}$$

The zeroth-order terms in Eq. (3) do indeed average to zero, leaving only first-order terms in $(\frac{a}{d})$. In this regime, the

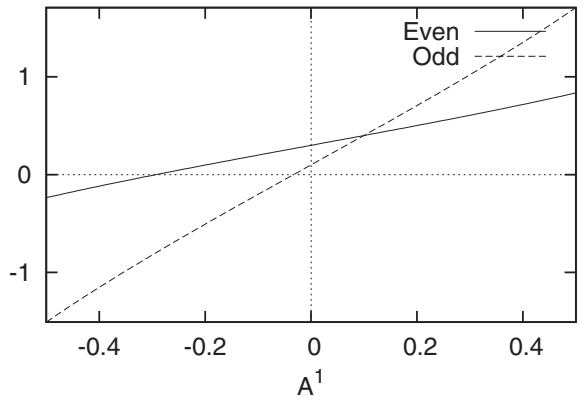

FIG. 3. Bracketed term, Eq. (7), for typical sets of parameters and for even and odd parity rotors.

hydrodynamic far-field contributions to stability from elastic deformation (finite k_r) and force perturbation (finite A^1) are of comparable magnitude. Once more, synchronization is promoted by elasticity, as represented by the first terms on the right. The second term derives from force modulation. It passes through the origin with a positive gradient and is locally linear. Providing the magnitude of the first term is not too great, the synchronization strength changes sign for a small, negative value of A^1; see Fig. 3.

Beneath this value the phase-locked state is stable and above it is the synchronized state. This is an apparently smooth transition. As it is approached, the growth rate of a deviation from equilibrium also approaches zero, allowing the phase difference between the rotors to meander.

The primary difference between even and odd parity rotors is in the weighting of the contributions of the two mechanisms. The role of trajectory deformation is three times weaker for counter-rotation than it is for corotation, and the influence of force perturbation is three times stronger. We note that this less-stringent stability criterion admits steady-state trajectories in which the phase difference, $\delta_{S/P}^{E/O}$, oscillates periodically about zero, providing its cycle average is zero. Similar such trajectories have been analyzed previously [22] and appear in experimental results.

Finally, we briefly consider the time periods and dissipation rates associated with each mode. Assuming zero disturbance from equilibrium ($\delta_{S/P}^{E/O} = 0$), integration of Eq. (3), $T = \int_0^{2\pi} \frac{d\phi}{\dot{\phi}}$, gives the time periods of each of the four modes:

$$T_{S/P}^{E} = \frac{2\pi\gamma R_0}{F_0\sqrt{1-(A^1)^2}}\left(1 \mp \frac{9}{8}\frac{a}{d}\right) \tag{8a}$$

$$T_{S/P}^{O} = \frac{2\pi\gamma R_0}{F_0\sqrt{1-(A^1)^2}}\left(1 \mp \frac{3}{8}\frac{a}{d}\right). \tag{8b}$$

The energy dissipated per cycle is $W_{S,P}^{E,O} = \int_0^T R_i F_\phi^i \dot{\phi}_i dt = \int_0^{2\pi} R_i F_\phi^i d\phi_i$. For sufficiently high radial stiffness the path deformation is only minor, $R_i \approx R_0$, and the energies of each mode converge to a single value, $W_{S,P}^{E,O} = W \approx 2\pi R_0 F_0$, for all modes. Under these conditions, the cycle averaged dissipation rates ($W_{S,P}^{E,O}/T_{S,P}^{E,O}$) are inversely proportional to the time periods, so that the synchronized states are the most efficient in this respect. For decreasing k_r, a more detailed treatment suggests that the efficiency advantage of synchronization is first degraded, then reversed. However, the substantial radial perturbations that are acquired by the rotors under these conditions, and the neglect of thermal fluctuations, which become increasingly significant, means that a more general approach would be required to properly treat the low k_r regime.

Comparing Eqs. (7) and (8) reveals that, for the set of four modes, the time periods and the contributions from each of the synchronization mechanisms are all evenly spaced and distinctively ordered. In particular, time periods are ordered, $T_S^E < T_S^O < T_P^O < T_P^E$. Furthermore, setting $A = 0$, gives $\Gamma_S^E < \Gamma_S^O < \Gamma_P^O < \Gamma_P^E$ for the synchronization strengths of rotors driven with constant torque, while putting $k_r = \infty$, yields $\Gamma_S^O < \Gamma_S^E < \Gamma_P^E < \Gamma_P^O$, for the ordering for rigidly tethered rotors, with $A > 0$.

IV. EXPERIMENTS AND SIMULATIONS

An experimental investigation of the system treated above has been conducted using holographic optical tweezers (HOT) to drive colloidal beads in the required manner. As has been described previously [26]. The parameters determining the system, the tangential force and its modulation amplitude (F_ϕ^i, A^1), and the radial stiffness, k_r, can be emulated with HOT. A force-clamping protocol [33] is used to produce the required tangential force, and position clamping [34] is used to generate the prescribed linear, radial restoring force. HOT control was performed using a modified version of the LabVIEW program detailed in Ref. [35].

Implementation of the force and position clamping procedures in HOT systems requires the accurate measurement of the coordinates of the beads followed by an update of the state of the spatial light modulator (SLM), so as to reposition the optical traps in such a way as to impose the required forces. This process introduces discrete time delays into the system. In order to approximate a continuous system, with the desired parameters (F_ϕ^i, A^1, k_r), the characteristic times of the system, including the effective relaxation times of the traps, must be substantially longer than these time delays. We ensure that this condition is satisfied by selecting the size of the beads we use and by controlling the viscosity of the ambient fluid, as described below. Other geometric parameters of the system, such as the size and separation of the oscillators, are constrained by the usable size of the field of view, and the requirement that the rotors be well separated from the container walls. As will be seen, the analysis captures the qualitative behavior of the system and provides satisfactory quantitative agreement. The moderate numerical disagreement can be attributed to the imperfections in the experimental system described above. To bridge the gap, we compare experiment with numerical integration of the basic equation of motion Eq. (2), using the scheme of Ermack and McCammon [36]. Idealized simulations reproduce analytical results, under the required assumptions ($a \ll d$, $R_0 \ll d$). Further, the time delays introduced by the feedback loop can be directly incorporated into the simulation, as can the thermal fluctuations, allowing direct comparison between simulation and experiment, and thereby indirect comparison between analysis and experiment.

Since synchronization strength cannot, itself, be directly measured, we concentrate on synchronization relaxation times. In direct analogy with standard methods of calibration for optical traps, equilibrium states of the rotors are considered to be bound by a fictitious potential. Since Γ gives the cycle-averaged growth rate of a particular disturbance, it evolves according to $\delta(i+1) - \delta(i) = \Gamma\delta(i)$, where i indexes the cycle, resulting in the relationship between relaxation time and synchronization strength:

$$\tau = \frac{-1}{\ln(1+\Gamma)} \approx \frac{-1}{\Gamma}. \tag{9}$$

For a pair of rotors, thermally fluctuating about a steady state, the relaxation time manifests itself as the decay time of the autocorrelation of the disturbance, $\delta^{E/O}_{S/P}$. The term on the far right, appropriate for $\Gamma \to 0$, describes the region in the vicinity of the transition and illustrates the qualitative interpretation of the synchronization strength as the reciprocal of the relaxation time, τ. It corresponds precisely to the solution of the continuous evolution, $\dot{\delta} = \Gamma\delta$.

It should be emphasized that this step is essentially heuristic. There is no *a priori* reason why a nonequilibrium thermodynamic process, such as colloidal synchronization, should be statistically similar to a system at thermodynamic equilibrium, such as a bead in a potential. Neither is it necessarily the case that the potentially complex restoration of synchrony, involving the combination of multiple relaxation processes, as indicated by the phase dependence of $\dot{\delta}/\delta$ in Eq. (5), should be well represented by a single, cycle-averaged relaxation. These issues are exaggerated in the case of phase-locked states, in which the range of $\dot{\delta}^{E/O}_P/\delta^{E/O}_P$ necessarily includes positive and negative values, and disturbances can grow before they decrease. However, as is amply demonstrated by the proceeding results, the protocol described above constitutes a meaningful measure of the time taken for a disturbance to return to steady state, even if the true physical complexity is concealed.

The parameters used in experiments were chosen in such a way as to facilitate both the conduction of the experiment, in terms of applying force and position clamping protocols, and the taking of measurements. In particular, we use solutions of glycerol to increase the fluid viscosity and slow down the dynamics in which we are interested, so that the discrete nature of the force and position clamping algorithms is smoothed out. Additionally, we use moderately large polystyrene beads of radius $a = 1.66\,\mu$m, to ensure accurate measurement of their coordinates. The beads are driven around circular paths of radius $R_0 = 2\,\mu$m to which they are bound by a radial stiffness, $k_r = 9.32\,\text{pN}/\mu\text{m}$, for even parity rotor pairs, and $k_r = 2.50\,\text{pN}/\mu\text{m}$ for odd pairs. Tangential forces are $F^1_0 = 3.85\,$pN for even parity and $F^1_0 = 5.37\,$pN for odd parity rotors. The rotor separation $d = 10\,\mu$m (Fig. 1) in both cases. Measurements are performed in a mixture of water and glycerol, with a viscosity of 0.24 Pas for even, and 0.19 Pas for odd parity. The viscosity of glycerol solution changes rapidly with concentration and temperature, making precise control difficult; the quoted values are measured experimentally *in situ* by measuring the autocorrelation of a bead in a static trap [26]. The rotors are separated from the nearest wall of the sample cell, by 50 μm. Beads are tracked by image processing of camera frames at 280 Hz, and trap positions are updated by an SLM with an update rate of 50 Hz, with new trap positions determined by current bead positions. An iterative calibration process is used to determine the size of the tangential steps taken by the optical traps, such that the desired force profiles, $F^i_\phi(\phi)$, are obtained. This is achieved by measuring the velocity profile, which is proportional to the force profile, of each rotor in isolation. The radial placement of each trap is proportional to the distance between the bead location and the defined trajectory, and the constant of proportionality scales the effective stiffness, k_r, of the radial force that acts to keep the bead on the defined trajectory. Autocorrelation function analysis is performed on Brownian trajectories of pairs of beads, after they have reached a steady state.

Figure 4 shows simulated and experimentally measured relaxation times, for even and odd pairs of rotors, as function of the amplitude of the force perturbation. Beneath these curves are shown experimental and simulation results for the equilibrium phase differences between the rotors. It appears that the transition between synchronized and phase-locked states is accompanied by a singularity in the relaxation time,

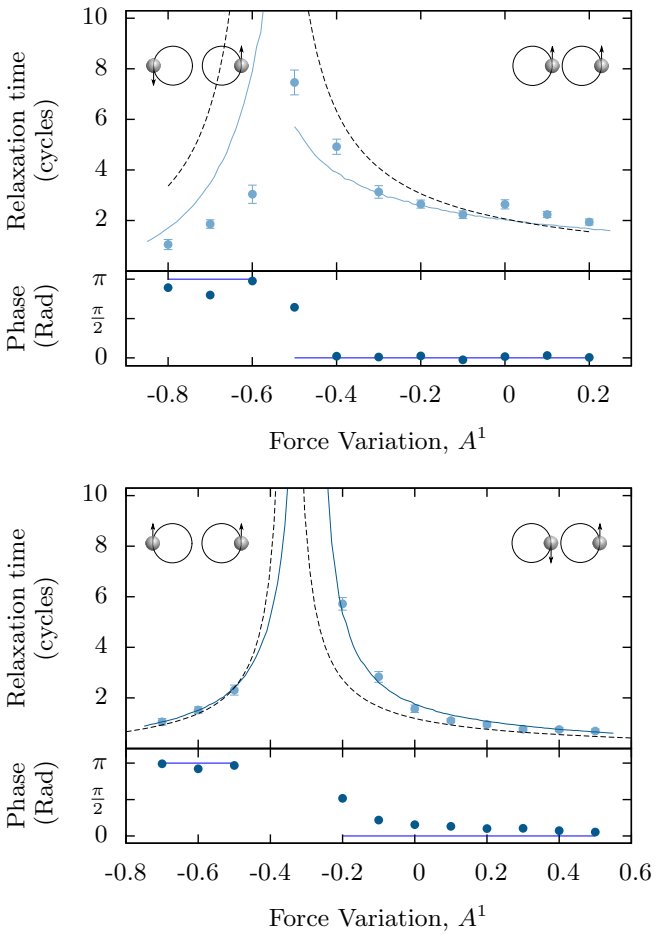

FIG. 4. (Color online) Graphs showing the variation of relaxation time with amplitude of force variation, A^1, for rotors of even (above), and odd parity (below). Experimental data is plotted as points and continuous lines show numerical results. The analytical approximation is shown by the dashed line.

as the synchronization strength approaches zero. However, accurate measurement of the relaxation time close to the singularity is challenging, and the details of the dynamics, as qualitatively discussed below, may become complicated. Hence, the interpretation of both numerical and experimental results becomes unclear in this region. It is evident, however, that the transition occurs for significant values of A, indicating that the force modulation mechanism does not completely dominate behavior in this regime, and the two identified mechanisms compete to determine behavior. Also shown Fig. 4 are analytically estimated relaxation times. As described above, for practical reasons, the experimental parameters do not conform precisely to the approximations made in the analysis. In particular, the ratio (a/d) is assumed small although, experimentally it is $\approx$0.17. Furthermore, the analysis omits the time delays associated with force and position clamping. Nevertheless, Eqs. (7) predict sensible values for the modulation amplitude, A^1, at which the transitions from synchronization to phase locking occur: -0.56 for the even rotors, -0.34 for odd. Additionally, estimates of the relaxation times, according to $\tau \approx -1/\Gamma$, are qualitatively consistent and quantitatively comparable with the experimental and numerical results.

Differences in the physical parameters used in the two sets of experiments makes direct comparison of measured time periods, with Eq. (8), complicated. However, it is incontrovertibly the case that synchronized states have lower time periods than phase-locked states. In addition, the influence of hydrodynamic coupling on time period is substantially greater for even parity rotors than it is for odd parity. In particular, measured time periods are $T_S^E \approx 20s$, $T_P^E \approx 30s$, $T_s^O \approx 13s$, and $T_p^O \approx 20s$.

V. CONCLUSIONS

To summarize, we have examined experimentally, numerically, and analytically the steady-state modes available to hydrodynamically coupled colloidal rotors circulating in the same sense (even parity rotors) and in opposing senses (odd parity). Attention is restricted to the hydrodynamic far field, in which the rotors are small compared with their separation. The rotors used are the simplest possible; colloidal beads harmonically bound to a circular path, with finite radial stiffness (k_r), and driven by phase-dependent tangential forces, $F_\phi = F_0[1 - A\sin(2\phi)]$. Experimental investigations are conducted using holographic optical tweezers to re-create the required conditions. Two independent mechanisms for synchronization have previously been identified. One relies on elastic deformation of the bead trajectory through finite radial stiffness (finite k_r), the other on modulation of the tangential force (finite A). We have shown that these mechanisms interact to determine behavior. Four equilibrium states have been identified. Each parity admits a synchronized state in which the phase difference (or sum, for odd parity), is zero, and a phase-locked state in which the phase difference (or sum), is π rads. The weighting of the two synchronization mechanisms determines which mode is selected, and this can be adjusted by varying the radial stiffness (k_r) or the amplitude of the force modulation (A). This is experimentally demonstrated by varying A between positive and negative values to induce a transition between synchronized and phase-locked states. Numerical simulations reproduce analytical results as well as experimental results when experimental nonidealities are incorporated.

Several conclusions can be drawn from this work. First of all, the previously identified synchronization mechanisms (finite k_r and finite A), are of comparable magnitude and can compete or cooperate to determine behavior, depending on A and k_r. Next, odd and even parity rotors admit both synchronized and phase-locked modes. Here we note that, for odd parity, counter-rotating rotors, these two states are reminiscent of the swimming strokes of the alga, Chlamydomonas. In particular, the phase locked mode is similar to the antiphase synchronization recently observed in mutant Chlamydomonas [14,15]. Although, these forms of synchrony are predominantly attributed to mechanical coupling [19,20], our results indicate that aspects of the observed behavior can be re-created through hydrodynamic interactions alone. While mechanical coupling is certainly the dominant mechanism, it apparently works in concert with hydrodynamics. In addition, analysis suggests that it is only the synchronized modes that can be uniformly stable in the sense that a small disturbance will be reduced for all phases in a cycle. In contrast, the phase-locked states can only be stable in a weaker sense, in which average disturbances are reduced over a complete cycle. Further, we have shown that the synchronized states lead to increased efficiency, in terms of energy dissipated into the ambient fluid, and that the stability of the modes, and therefore their robustness against thermal effects, can be increased via the force modulation amplitude, A. These insights could assist in determining effective ways of driving biomimetic microfluidic devices [31].

A number of new questions present themselves. For example, in common with other existing studies, we have remained in the hydrodynamic far field. In this regime, the two synchronization mechanisms (finite A, finite k_r) appear distinct, so that their weights can be adjusted independently. The extent to which this remains true for large, proximal rotors is unclear. Similarly, the stability conditions for each of the four states described above appear mutually exclusive, in that there is no apparent bistability. Were this to break down in the near field, one would expect to see a variety Kramers hopping between nonequilibrium states or, given a higher thermal barrier, hydrodynamic hysteresis. Although not presented here, simulations of rotors close to the transition between synchronization and phase-locking appear to show such behavior, even in the far field. Finally, we note that the nature of synchronization mechanisms studied here derives from the symmetry of the rotors. However, the way in which these processes are modified by reductions in rotor symmetry is yet to be fully understood [37].

ACKNOWLEDGMENTS

S.S. was supported by the Ministry of Education, Youth and Sports of the Czech Republic (Project No. L01212). S.B. and L.D. were supported by EPSRC (U.K.). Experimental and numerical work was conducted within the Bristol Centre for Nanoscience and Quantum Information, and the Advanced Computing Research Centre, University of Bristol.

[1] S. H. Strogatz, Physica D: Nonlinear Phenomena **143**, 1 (2000).
[2] Y. Kuramoto, *Chemical Oscillations, Waves, and Turbulence* (Courier Dover Publications, New York, 2003).
[3] F. K. Lamb, J.-J. Aly, M. C. Cook, and D. Q. Lamb, Astrophys. J. **274**, L71 (1983).
[4] A. D. Aczel, Sci. Am. **304**, 30 (2011).
[5] B. S. Kerner and H. Rehborn, Phys. Rev. Lett. **79**, 4030 (1997).
[6] A. Sansone and G. Garofalo, Physica A: Stat. Mech. Appl. **382**, 247 (2007).
[7] E. Lauga and T. R. Powers, Rep. Prog. Phys. **72**, 096601 (2009).
[8] C. Brennen and H. Winet, Annu. Rev. Fluid Mech. **9**, 339 (1977).
[9] R. Golestanian, J. M. Yeomans, and N. Uchida, Soft Matter **7**, 3074 (2011).
[10] M. Reichert and H. Stark, Eur. Phys. J. E: Soft Matter Biol. Phys. **17**, 493 (2005).
[11] A. Vilfan and F. Jülicher, Phys. Rev. Lett. **96**, 058102 (2006).
[12] J. Gray, Proc. Roy. Soc. London Ser. B **9**, 313 (1930).
[13] M. J. Sanderson and M. A. Sleigh, J. Cell Sci. **47**, 331 (1981).
[14] K. Y. Wan, K. C. Leptos, and R. E. Goldstein, J. R. Soc. Interface **11**, 20131160 (2014).
[15] K. C. Leptos, K. Y. Wan, M. Polin, I. Tuval, A. I. Pesci, and R. E. Goldstein, Phys. Rev. Lett. **111**, 158101 (2013).
[16] M. Polin, I. Tuval, K. Drescher, J. P. Gollub, and R. E. Goldstein, Science **325**, 487 (2009).
[17] Y. W. Kim and R. R. Netz, Phys. Rev. Lett. **96**, 158101 (2006).
[18] J. Elgeti and G. Gompper, Proc. Natl. Acad. Sci. USA **110**, 4470 (2013).
[19] V. F. Geyer, F. Jülicher, J. Howard, and B. M. Friedrich, Proc. Natl. Acad. Sci. USA **110**, 18058 (2013).
[20] B. M. Friedrich and F. Jülicher, Phys. Rev. Lett. **109**, 138102 (2012).
[21] N. Bruot, J. Kotar, F. de Lillo, M. Cosentino Lagomarsino, and P. Cicuta, Phys. Rev. Lett. **109**, 164103 (2012).
[22] N. Uchida and R. Golestanian, Eur. Phys. J. E **35**, 135 (2012).
[23] M. Theers and R. G. Winkler, Soft Matter **10**, 5894 (2014).
[24] T. Niedermayer, B. Eckhardt, and P. Lenz, Chaos: Interdisc. J. Nonlin. Sci. **18**, 037128 (2008).
[25] N. Uchida and R. Golestanian, Phys. Rev. Lett. **106**, 058104 (2011).
[26] J. Kotar, L. Debono, N. Bruot, S. Box, D. Phillips, S. Simpson, S. Hanna, and P. Cicuta, Phys. Rev. Lett. **111**, 228103 (2013).
[27] R. R. Bennett and R. Golestanian, Phys. Rev. Lett. **110**, 148102 (2013).
[28] P. Lenz and A. Ryskin, Phys. Biol. **3**, 285 (2006).
[29] K. Drescher, R. E. Goldstein, N. Michel, M. Polin, and I. Tuval, Phys. Rev. Lett. **105**, 168101 (2010).
[30] J. S. Guasto, K. A. Johnson, and J. P. Gollub, Phys. Rev. Lett. **105**, 168102 (2010).
[31] A. Shields, B. Fiser, B. Evans, M. Falvo, S. Washburn, and R. Superfine, Proc. Natl. Acad. Sci. USA **107**, 15670 (2010).
[32] S. Kim and S. J. Karrila, *Microhydrodynamics: Principles and Selected Applications* (Courier Dover Publications, New York, 2013).
[33] D. Phillips, G. Gibson, R. Bowman, M. Padgett, S. Hanna, D. Carberry, M. Miles, and S. Simpson, Opt. Express **20**, 29679 (2012).
[34] D. Phillips, S. Simpson, J. Grieve, G. Gibson, R. Bowman, M. Padgett, M. Miles, and D. Carberry, Opt. Express **19**, 20622 (2011).
[35] R. W. Bowman, G. M. Gibson, A. Linnenberger, D. B. Phillips, J. A. Grieve, D. M. Carberry, S. Serati, M. J. Miles, and M. J. Padgett, Comput. Phys. Commun. **185**, 268 (2014).
[36] D. L. Ermak and J. McCammon, J. Chem. Phys. **69**, 1352 (1978).
[37] A. V. Arzola, P. Jákl, L. Chvátal, and P. Zemánek, Opt. Express **22**, 16207 (2014).